University of Auckland

Advanced Physics Laboratory

Experiment 343

Compton Scattering Relativistic Electrons

Shalini Srinivasan
ssri261
Student ID: 655069553

September 15, 2022

1 Introduction

At a time when the wave-particle duality of light was still being accepted, Arthur Compton's discovery of the Compton effect was a much needed proof toward the particle nature of light. Compton studied the behaviour of x-rays scattering electrons and asserted that they must have particle like properties for the unexpected behaviour to be explained.

Under the assumption, 'photons are waves', the expectation was x-rays would cause electrons to forced into vibrating at the same frequency and result in according radiation. However, when the experiment is carried out the observations were unexpected and the behaviours difficult to explain with the current assumptions.

The three areas explored here are; Compton kinematics (the Energy-Angle relationship), Compton cross-section (probability of scattering), relativistic electrons.

In the final section we take advantage of the high speed electrons produced in this experiment to show the behaviour of electrons at high speeds.

2 Compton Kinematics

Compton scattering of a gamma ray of an electron results in a shift in the wavelength. This is an important discovery as it means photons can be treated as particles. The relationship can be derived using the conservation laws, and taking the gamma spectrum at various angles will test the predicted relationship. Compton Equation (Equation 1)

$$\frac{1}{E'_\gamma} - \frac{1}{E_\gamma} = \frac{1}{m_0 c^2}(1 - \cos\theta) \text{eq 1} \qquad (1)$$

2.1 Method

First adjust the amplifier of the detector such that the 137Cs photo-peak will stay displayed as we change the scattering angle (namely between the source direction and the detector) and calibrate the analyser.

Using a flat scatterer save the resulting spectrum over a range of angles to find the effect of angle on the energy. Ideally measure on both sides to reduce error in the angle, but this was skipped to due lack of time.

(Note: The scatterer should be placed such that the material travelled is a minimum.)

Repeat with another scatterer at specific angles.

2.2 Results & Discussion

θ	20	40	60	80
$\frac{1}{E'_\gamma}$	1.65±0.01	2.00±0.05	2.55±0.08	3.23±0.08

θ	100	120	139
$\frac{1}{E'_\gamma}$	3.90±0.07	4.55±0.07	5.25±0.8

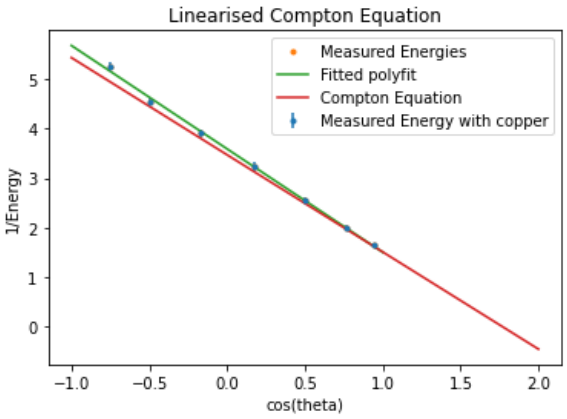

Plotting $\frac{1}{E'_\gamma}$ against $\cos\theta$ gives a linear plot with the equation.

$$\frac{1}{E'_\gamma} = m\cos\theta + c$$

gradient	-2.082 +/- 0.002
constant	3.587 +/- 0.001

Compton Equation predicts the following,

$$\frac{1}{E'_\gamma} = \frac{-1}{m_0 c^2}\cos\theta + \left(\frac{-1}{m_0 c^2} + \frac{1}{E_\gamma}\right)$$

,where $m_0 c^2$ is the rest mass energy of an electron and E_γ is the energy of the gamma rays from the ^{137}Cs source (0.611 MeV).

So the expected coefficients are,

gradient	-1.957
constant	3.594

The fitted coefficients are off by 0.125 and 0.007, this is enough to conclude that the experimental results map to the prediction despite the error being greater than polyfit gives. Looking at the plot it can be seen that the measurement at 139^o does not match up to the prediction at all unlike the other points. The angle is likely larger than initially observed. This is probably why we see the true values falling outside the uncertainty, though polyfit does seem to be underestimating the error.

- **Q1: Aluminium vs Copper Scatterer**
  Comparing the 2 sets of data, for copper

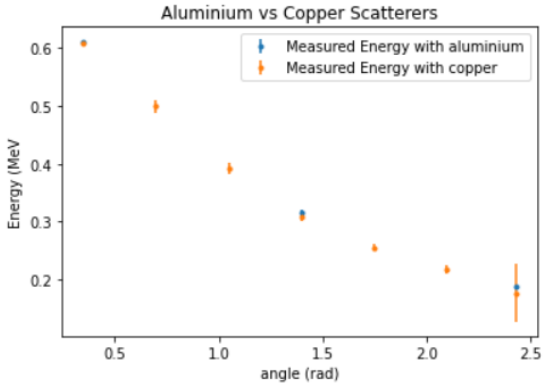

  and aluminium they have minimal variance so it can be concluded that it does not affect the results. This is to be expected as the ray's energy depends solely on angle.

- **Q2: Spectrum Peaks**
  Using the Cesium spectrum from the calibration, The peak around channel 4000

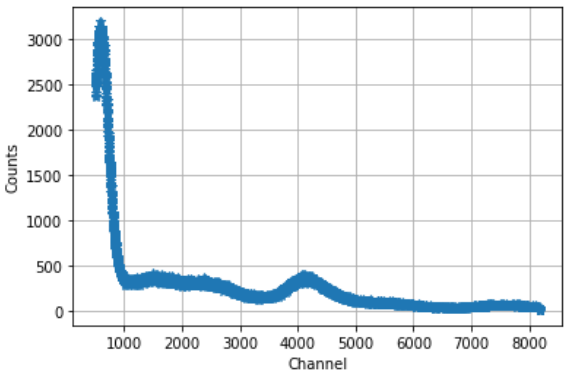

  is the photo-peak of energy 0.662 MeV. At the very left, a large peak (after the first peak caused by the detector which has been left out of this) can be seen around channel 500 which is the photo-peak of energy 0.031 MeV. There are 2 smaller peaks that can be seen between the previously mentioned. The right peak is the Compton edge of the 0.662 MeV photo-peak. The left may be due to backscatter from gamma rays hitting the material surrounding the crystal then being detected.

3 Compton Cross Section

In this section we compare the classical and quantum mechanical predictions of the probability of scattering, called 'cross-section'. In particular the probability of detecting a scattered photon at a particular angle of an infinitesimal angle element. When the energy of the photon is greater than the electron rest energy, they interact and the photon loses energy in inelastic scattering.

This part compares the Thompson classical prediction,

$$\frac{d\sigma}{d\Omega} = r_o^2 \left(\frac{1+\cos\theta^2}{2} \right) \tag{2}$$

,to the Klein-Nishina quantum mechanical prediction,

$$\frac{d\sigma}{d\Omega} = r_o^2 \left(\frac{1+\cos\theta^2}{2} \right) \frac{1}{[1+\gamma(1-\cos\theta)]^2} \left(1 + \frac{\gamma^2(1-\cos\theta)^2}{(1+\cos\theta^2)[1+\gamma(1-\cos\theta)]} \right) \tag{3}$$

3.1 Method

The same data collected from the Compton Kinematics section above is applicable here too. The angle being between the source direction and the detector.

Due to peaks merging it was not possible to sum counts over all of the peak and compare. So instead a small section centered at each peak (800 channels) was summed over. Then using the count at 20^{deg} as 90% of the total count we get a probability.

Other things accounted for; detector efficiency (14% for ^{137}Cs source (0.611 MeV)), the amount of scatterer material travelled ($\cos\theta/2$ for $\theta < 90$ and $\cos(\pi-\theta)/2$ for $\theta > 90$).

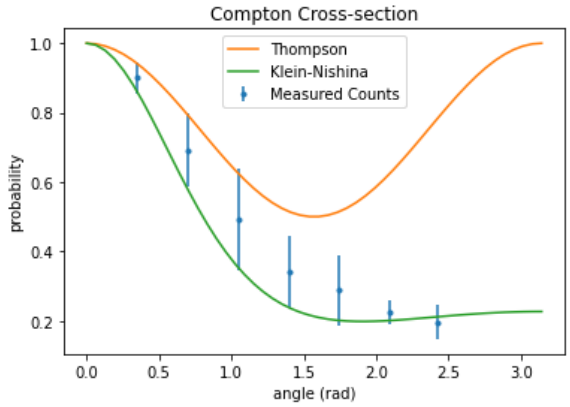

3.2 Results & Discussion

As we can see in the figure, the Klein-Nishina predicts the experimental result more accurately compared to the Thompson as expected. It is clear that most gamma rays are scattered at very forward angles.

For the uncertainty it was difficult to decide what to base it on. In the end, a subjective method was chosen. By looking at the data of the peaks a relative uncertainty was assigned to each based on what percent of the peak had merged into another and on how much the data clustered around the Gaussian fit. (Refer to the plots at the end).

4 Relativistic energy-momentum relations

Newtonian mechanics fails at high speeds where we must apply special relativistic principles instead. In this lab we look specifically at the relationship between momentum and kinetic energy of particles. The classical prediction states,

$$\frac{P^2}{2m_o} = T \tag{4}$$

whereas special relativity states energy to be $E = T + m_o c^2$, it accounts for the rest mass energy of a particle. As such energy and momentum are related by,

$$E^2 = P^2c^2 + m_o^2c^4 \tag{5}$$

$$\frac{P^2}{2m_o} = T + \frac{T^2}{2m_oc^2} \tag{6}$$

Using momentum conservation, $P_e = \frac{1}{c}(E_\gamma + E'_\gamma)$ we get the momentum of the electron to be,

$$P_e = \tfrac{1}{c}(2E_\gamma - T_e) \tag{7}$$

Under relativistic speeds the mass is more accurately given by,

$$m = \frac{m_o}{\sqrt{1-\frac{v^2}{c^2}}} \tag{8}$$

where m_o is the rest mass of the electron ($0.511\text{MeV}/\text{c}^2$)

The event when a gamma ray collides head on with an electron is when maximum electron kinetic energy is seen. This is then used to find momentum.

4.1 Method

Following the same method as the calibration, take the gamma spectrum for multiple sources. The sources used in this section are; Americium, Barium, Bismuth, Cesium, Europium, and Sodium.

The photo-peak gives the photon energy while using the Compton edge we can estimate where the maximum electron kinetic energy falls.

4.2 Results & Discussion

For the uncertainty it was assumed the value would be within the middle 50% of the Compton edge range so the uncertainty was set to be about a $\frac{1}{4}$ of the Compton range.

	Americium	Barium	Bismuth
T_e	0.030 ±0.006	0.20 ±0.01	0.40 ±0.03
$\frac{P^2}{2m_o}$	0.008 ±0.002	0.26 ±0.02	0.55 ±0.05
γ	1.0 ±0.2	1.4 ±0.1	1.8 ±0.2
β	0.18 ±0.04	0.71 ±0.05	0.82 ±0.07

	Cesium	Europium	Sodium
T_e	0.49 ±0.03	0.26 ±0.02	0.33 ±0.03
$\frac{P^2}{2m_o}$	0.68 ±0.05	0.18 ±0.01	0.47 ±0.05
γ	1.9 ±0.1	1.3 ±0.1	1.7 ±0.2
β	0.85 ±0.06	0.64 ±0.05	0.81 ±0.09

Looking at the following plots it can be seen that the bismuth and americium source (3rd, 1st data points), especially bismuth, don't quite behave as expected but overall the other

four sources follow the special relativity predictions closely and in these cases the uncertainty chosen was more than necessary. Reducing the uncertainty for these to be within the middle 25% of the edge would be a safe assumption.

4.2.1 Experimental Momentum

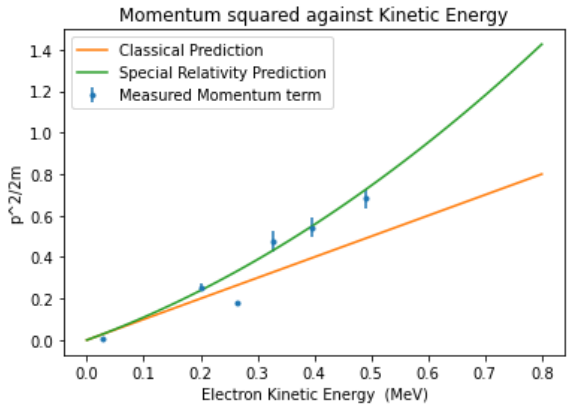

Considering bismuth an outlier, as expected the experimental momentum closely follows the special relativity prediction.

4.2.2 Experimental Mass Variation

From equation 7 we can see that the mass variation will be given by γ, the Lorentz factor. By multiplying the mass variation by $\frac{c^2}{c^2}$ we get that can be calculated experimentally,

$$\gamma = \frac{E_e}{m_o c^2} \tag{9}$$

The variation in mass goes up linearly as the

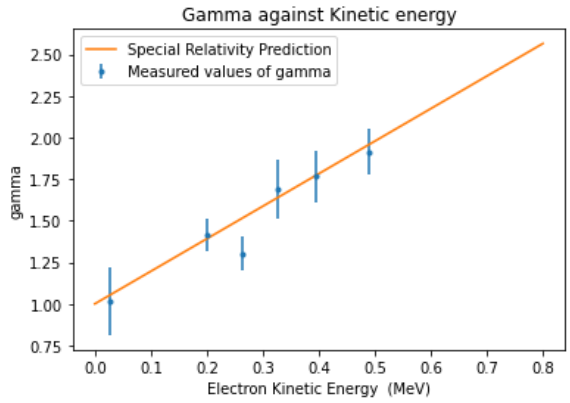

kinetic energy increases like the prediction.

4.2.3 Experimental Speed

Here the Lorentz factor is used to solve for β, this is a measure of the speed as a fraction of the speed of light.

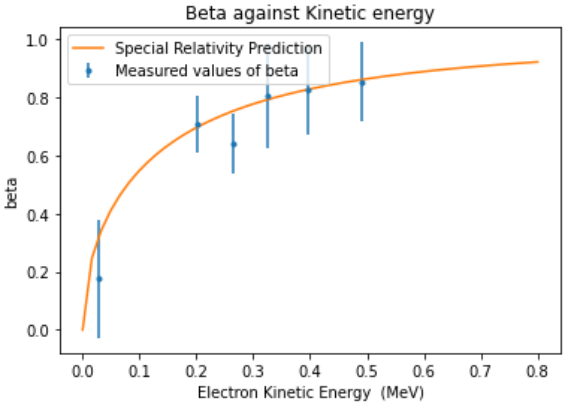

It can be seen that the measurements follow the prediction and plateaus as the speeds approaches the speed of light and can not pass it.

- **Q3: Derivations**

- Equation 4
  Knowing that total electron energy, E_e, is given by $E_e = T_e + m_0c^2$ and that E_e and momentum, P_e, are related by, $E_e^2 = P_e^2c^2 + m_0c^2$ (eq. 3) we can find an expression for P_e and kinetic energy, T_e;

$$E_e^2 = T_e^2 + 2T_em_0c^2 + m_o^2c^4$$

  , setting this equal to eq. 3 we can see that the $m_o^2c^4$'s will cancel leaving us with,

$$T_e^2 + 2T_em_oc^2 = P_e^2c^2$$

  , dividing through by $2m_0c^2$ gives the desired relation.

$$\frac{P_e^2}{2m_o} = T_e + \frac{T_e^2}{2m_oc^2}$$

- Equation 9
  The mass variation given by, $\gamma = \frac{m}{m_o} = \frac{E_e}{m_oc^2}$. Then using equation 5

(

$\mathrm{E}^2 = P^2c^2 + m_o^2c^4)and using equation 7, \mathrm{P}_e = \frac{1}{c}(2E_\gamma - T_e)$, the following is derived.

  First square equation 7

$$P_e^2 = \frac{1}{c^2}(2E_\gamma - T_e)^2$$

  ,putting this into equation 5 and square-rooting gives the following expression for E_e,

$$E_e = \left[(2E_\gamma - T_e)^2 + m_o^2c^4\right]^{1/2}$$

  ,finally dividing everything by m_oc^2 gives the mass variation and therefore γ.

$$\frac{[(2E_\gamma - T_e)^2 + m_o^2c^4]^{1/2}}{m_oc^2}$$

$$\gamma = \frac{E_e}{m_oc^2} = \left[\left(\frac{2E_\gamma - T_e}{m_oc^2}\right)^2 + 1\right]^{1/2}$$

$$\gamma = \frac{E_e}{m_oc^2} = \left[\left(\frac{2E_\gamma - T_e}{m_oc^2}\right)^2 + 1\right]^{1/2}$$

- Equation 11
  Using equation 7, $P_e = \frac{1}{c}(2E_\gamma - T_e)$

$$P_e^2 = \frac{(2E_\gamma - T_e)^2}{^2c}$$

  ,divide through by $2m_o$ to get the desired relation,

$$\frac{P_e^2}{2m_o} = \frac{(2E_\gamma - T_e)^2}{2m_oc^2}$$

- **Experimental** γ Consider the propagation of uncertainty of the following two equivalent equations for γ,

$$\gamma = \left[\left(\frac{2E_\gamma - T_e}{m_oc^2}\right)^2 + 1\right]^{1/2}$$

  VS

$$\gamma = \left(\frac{(2E_\gamma - T_e)^2}{m_oc^2}\right)^2 - 1$$

  It is simplest to consider the relative uncertainty (let this be called rel). In these equation only the exponents will affect the relative uncertainty (uncertainty will be scaled by the value of the exponent ie. multiplied) as everything else is an exact value. So to find the result uncertainty instead consider the two equations following,

$$\sigma = (rel^2)^{1/2} = rel * 2 * \frac{1}{2} = rel$$

$$\sigma = (rel^2)^2 = rel * 2 * 2 = 4 * rel$$

  Clearly, the preferred equation is the first as the uncertainty is lower, in fact it is (relatively) unchanged. This is definitely preferred to the second which is quadrupled.

- **Sodium Iodide Scintillation Crystal** The larger the scintillation crystal is, the more photons that will be captured and detected. This makes the edge less distinct which is why a smaller crystal is preferred so that more photons escape, displaying a more obvious edge.

- **Kinetic Energy** Ideally we would see a sharp cut off as the compton edge giving us an exact value for the point of max kinetic energy. However, due to detector efficiency we instead see a more fuzzy compton edge, likely due to some photons at angles around 180^o also escaping detection. So assuming there is a fairly symmetrical number of photons above and below the 180^o photons escaping the T_e was taken to be the middle of the edge and the uncertainty was based on the assumption the max energy would be within the middle 50% ie. $\pm 25\%$.

- ^{60}**Cobalt** Cobalt-60 was not used due partially to the low detector efficiency at those high energies (1.173 MeV, 1.333 MeV) but mainly as the detector resolution is not high enough to differentiate these peaks properly so will merge on the display.

- ^{207}**Bismuth** Bismuth-207 gives a reliable peak at 0.075 MeV that can be used for calibration. However, this is not a gamma ray but in fact an x-ray. Bismuth-207 decays to lead which then produces Pb-K x-rays. X-rays are simply photons so will get detected along with the gamma rays.

5 Conclusion

This was the an extremely interesting lab that showcased many important behaviours of photons that just can not be explained by the wave nature of photons. This lab was also useful in learning how to work with large data sets and analyse the areas of interest.

6 References

1. www.overleaf.com
2. Crucial Experiments in Modern Physics, George L. Trigg
3. Experiments in Modern Physics, Hans Mark, N. Thomas Olsen
4. Compton effect, https://www.britannica.com/science/radiation/Cross-section-and-Compton-scattering
5. Gamma Spectrum, https://www.radiochemistry.org/periodictable/gamma$_s pectra/Photopeakhttps$: $//www.radiation-dosimetry.org/what-is-photopeak-spectrum-definition/$
6. Cross-section, https://www.nuclear-power.com/nuclear-power/reactor-physics/interaction-radiation-matter/interaction-gamma-radiation-matter/compton-scattering/cross-section-compton-scattering/
7.
8. Compton Edge, https://www.radiation-dosimetry.org/what-is-compton-edge-definition/
9. Compton Edge, https://www.youtube.com/watch?v=dyYAnOOC51E
10. Compton Edge, https://www.nuclear-power.com/nuclear-engineering/radiation-detection/gamma-spectroscopy/what-is-compton-continuum-compton-plateau-spectrum/
11. Max kinetic energy, https://www.youtube.com/watch?v=jwdHudbF0mE
12. https://1.bp.blogspot.com/-Qbecu7hSO9g/Xzv3Gkx157I/AAAAAAAACMo/I5mQanetg2Mg77$_0 imCb0LlLlgdrAm_V gCLcBGAsYHQ/s2048/Eu-152_S pectrum.jpg$
13. Bismuth Decay, https://www.radiochemistry.org/periodictable/gamma$_s pectra/pdf/bi207.pdf$
14. Python Documentation

7 Data

7.1 Scattered: Copper

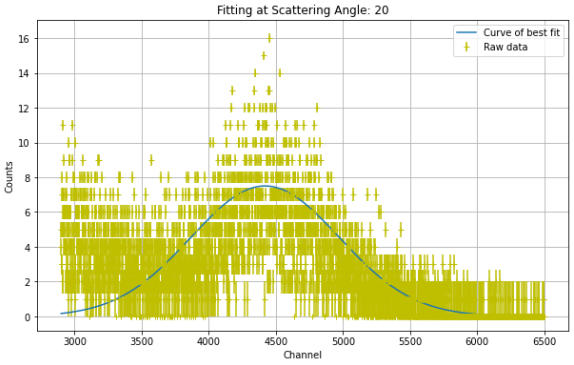

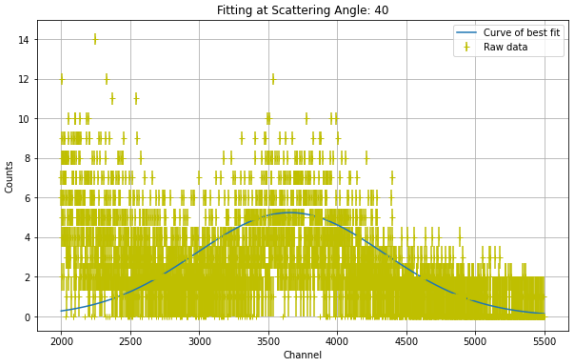

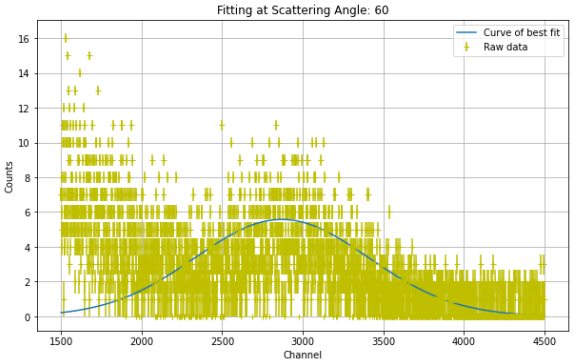

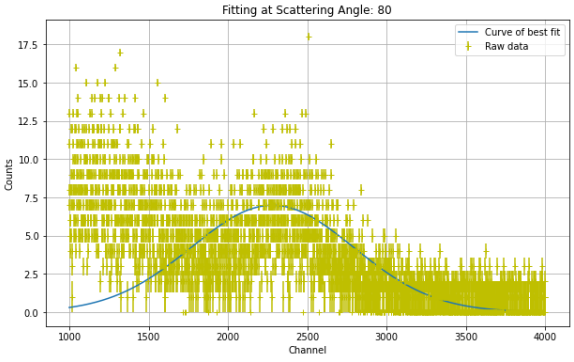

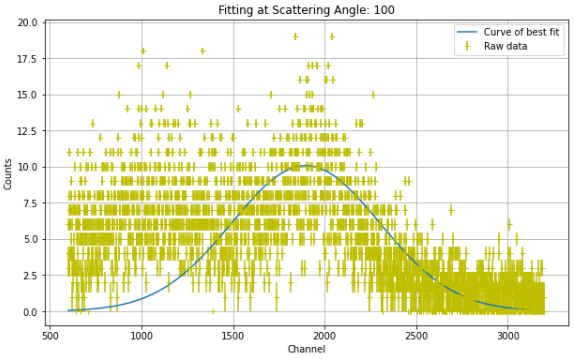

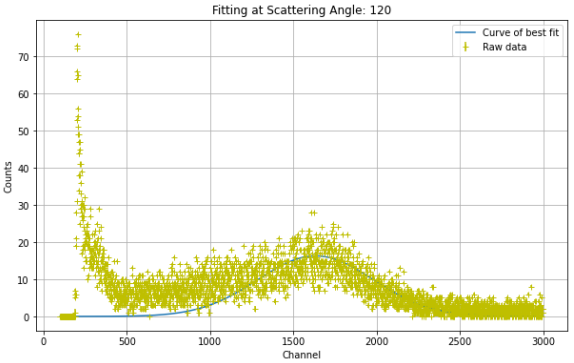

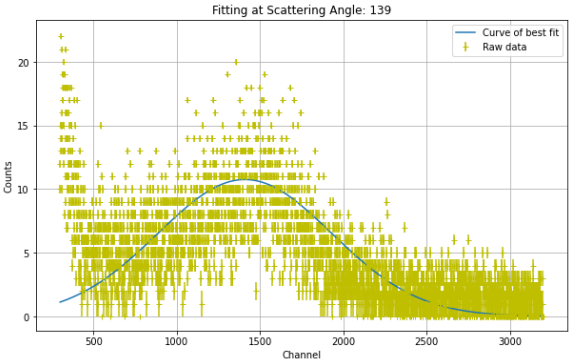

7.1.1 Scattered: Aluminium

A few test angles using a different scatterer.

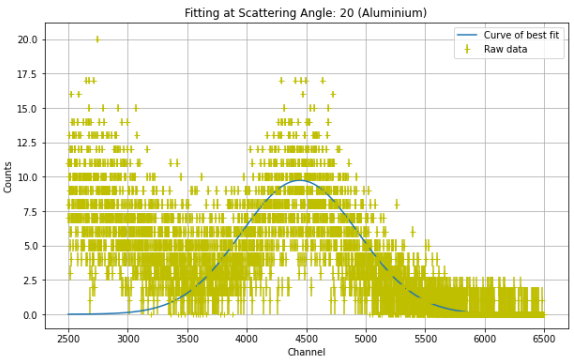

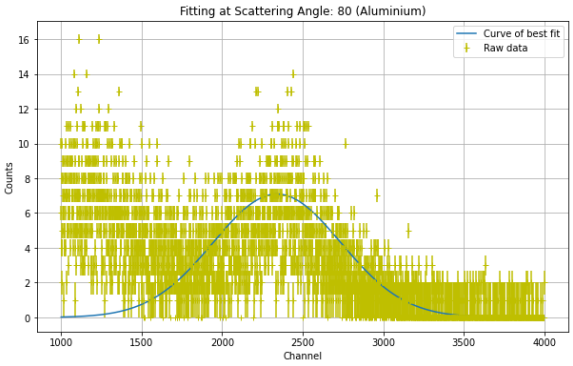

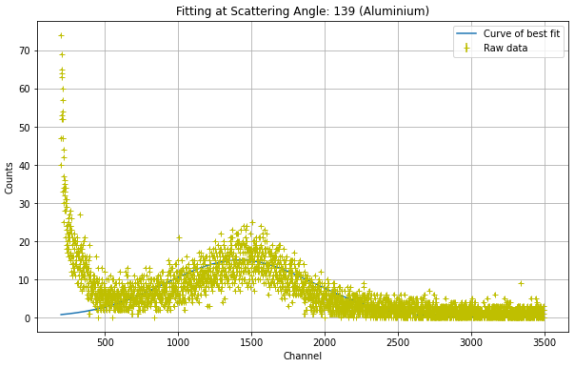

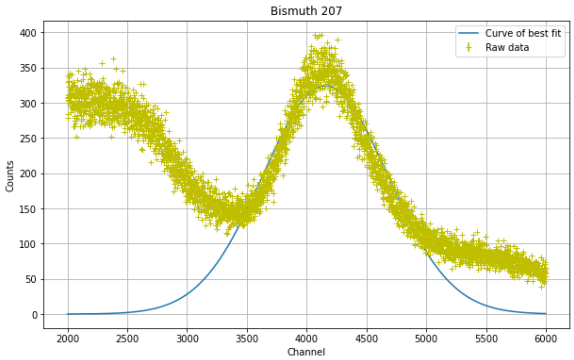

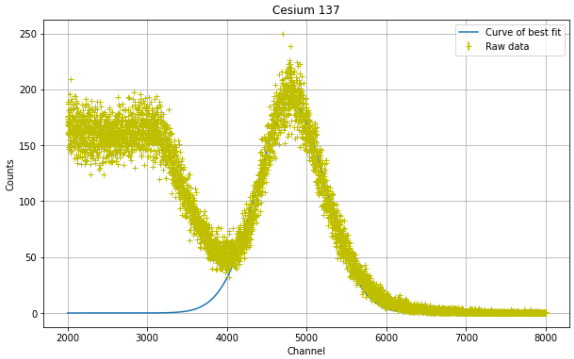

7.2 Sources: Compton Edge